



# The syntheses and photophysical properties of 4,4'-isopropylidendioxydiphenyl substituted ball-type dinuclear Mg(II) and Zn(II) phthalocyanines

MevlÜde Canlıca<sup>a,b</sup>, Tebello Nyokong<sup>b,\*</sup>

<sup>a</sup>Yildiz Technical University, Chemistry Department, Inorganic Chemistry Division, Davutpasa Campus, 34220 Esenler, Istanbul, Turkey

<sup>b</sup>Rhodes University, Chemistry Department, P.O. Box 6140, Grahamstown, South Africa

## ARTICLE INFO

### Article history:

Received 3 April 2011

Accepted 24 October 2011

Available online 2 November 2011

### Keywords:

Mg ball-type phthalocyanine

Zn ball-type phthalocyanine

Photodynamic therapy

Non-peripheral phthalocyanine

Triplet quantum yield

## ABSTRACT

The syntheses of ball-type dinuclear Zn(II) and Mg(II) phthalocyanines containing four 4,4'-isopropylidendioxydiphenyl substituents at the peripheral and non-peripheral positions are presented. The structures of the synthesized compounds were characterized using elemental analyses, and UV-Vis, FT-IR, <sup>1</sup>H NMR and mass spectroscopies. The  $\Phi_F$  values were 0.14, 0.11, 0.22, 0.15 and  $\Phi_T$  values were 0.84, 0.88, 0.62, 0.74, for **6–9**, respectively. The largest triplet yields were observed for the non-peripherally substituted complexes **6** and **7**, showing that non-peripheral substitution favors increased population of the triplet state. All complexes showed reasonably long triplet lifetimes with  $\tau_T$  510, 310, 910 and 350  $\mu$ s in DMSO, respectively.

© 2011 Elsevier Ltd. All rights reserved.

## 1. Introduction

Metallophthalocyanines (MPcs) have been studied as materials for many applications including in electronics [1], non-linear optics [2], liquid crystals [3], gas sensors [4], photosensitizers [5,6], electrocatalysis [7], semiconductors [8] and photovoltaic cells [9]. There is considerable interest in MPC complexes containing non-transition metals for use as photosensitizers in the relatively new method of cancer treatment called photodynamic therapy (PDT) [5,6,10–14]. The mode of operation in PDT is based on visible light excitation of a tumor-localized photosensitizer. After excitation, energy is transferred from the photosensitizer (in its triplet excited state) to ground state oxygen (<sup>3</sup>O<sub>2</sub>), forming excited singlet state oxygen (<sup>1</sup>O<sub>2</sub>). High triplet state quantum yields and long triplet lifetimes are required for efficient photosensitization. Syntheses, electrochemical and spectroelectrochemical behavior of ball-type Pc derivatives have been extensively studied since the complexes were published in the literature for the first time in 2002 [15,16]. Ball-type phthalocyanine derivatives show spectroscopic and electrochemical properties which differ significantly from the parent monomer [17–19]. However, the studies on non-peripherally substituted ball-type MPC derivatives are still limited and the photophysical behavior of ball-type molecules in general have also not received much attention. Our interest in ball-type complexes is due to the possibilities of intramolecular interactions between the Pc rings and/or metal centers of these compounds. The electronic

properties of ball-type Pcs can change dramatically depending on the bridging compounds or the central metal. The distance between the two Pc units affect the degree of interactions between the rings. In this paper, we describe the syntheses and photophysical properties of new symmetrically substituted ball-type MgPc and ZnPc complexes containing substituents at the non-peripheral ( $\alpha$ ) and peripheral ( $\beta$ ) positions, Scheme 1.

## 2. Experimental

### 2.1. Materials

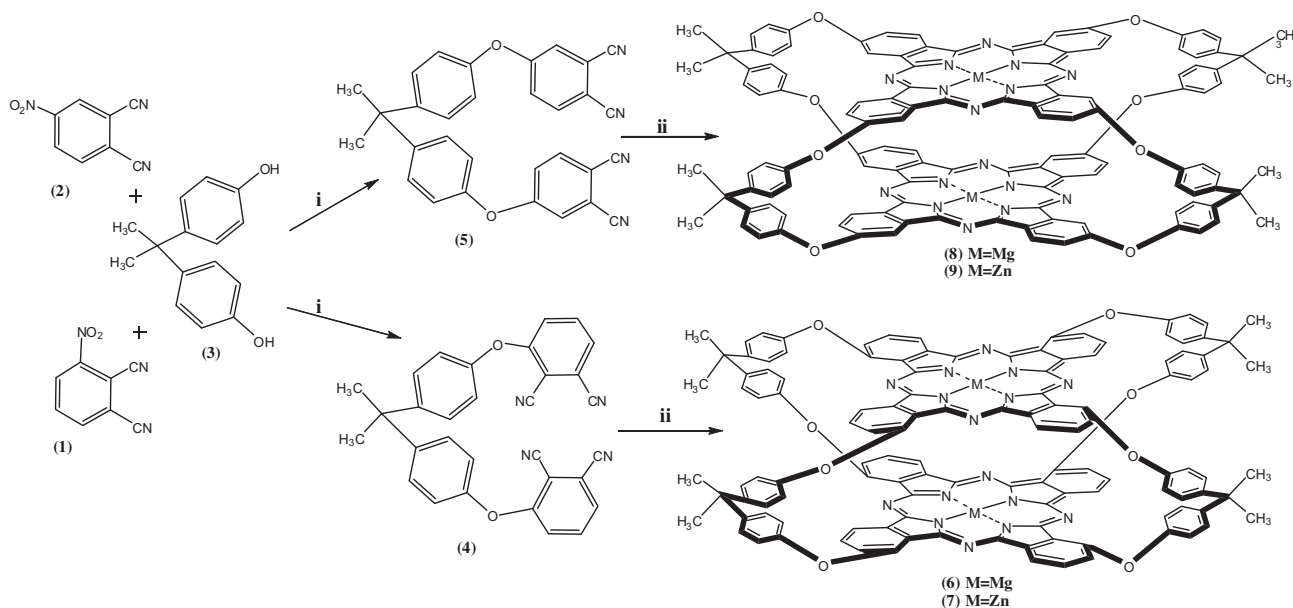
Anhydrous magnesium(II) chloride and zinc(II) acetate were purchased from Sigma-Aldrich. All solvents for example dimethylsulfoxide (DMSO) and chloroform were from Saarchem. Silica gel for column chromatography was purchased from MERCK. All other reagents were obtained from suppliers and used as received.

### 2.2. Equipment

UV-Vis absorption spectra were obtained using the Varian Cary 500 UV-Vis/NIR spectrometer. Fluorescence excitation and emission spectra were recorded with Varian Eclipse spectrophotometer. FT-IR data were recorded using the Perkin-Elmer spectrum 2000 FTIR spectrometer. <sup>1</sup>H NMR spectra were obtained using a Bruker EMX 400 MHz spectrometer. Elemental analyses were done on a Vario-Elementar Microcube EL III. Mass spectral data were collected with a Bruker AutoFLEX III Smartbeam MALDITOF/TOF Mass spectrometer. The instrument was operated in positive ion mode

\* Corresponding author. Tel.: +27 46 6038260; fax: +27 46 6225109.

E-mail address: [t.nyokong@ru.ac.za](mailto:t.nyokong@ru.ac.za) (T. Nyokong).



**Scheme 1.** Non-peripherally and peripherally substituted ball-type metallophthalocyanines. i: DMSO, rt, 5 days. ii: MgCl<sub>2</sub>, 450 °C, 15 min for **6,8** and Zn(CH<sub>3</sub>COO)<sub>2</sub>, 300 °C, 12 min for **7,9**.

using an  $m/z$  range of 400–3000. The voltage of the ion sources were set at 19 and 16.7 kV for ion sources 1 and 2, respectively, while the lens was set at 8.50 kV. The reflector 1 and 2 voltages were set at 21 and 9.7 kV, respectively. The spectra were acquired using dithranol as the MALDI matrix and a 354 nm nitrogen laser. Triplet absorption and decay kinetics were recorded on a laser flash photolysis system, the excitation pulses were produced by a Quanta-Ray Nd: YAG laser providing 400 mJ, 9 ns pulses of laser light at 10 Hz, pumping a Lambda-Physic FL 3002, dye (Pyridin 1 in methanol). The analyzing beam source was from a Thermo Oriol xenon arc lamp, and a photomultiplier tube was used as a detector. Signals were recorded with a two-channel 300 MHz digital real-time oscilloscope (Tektronix TDS 3032C); kinetic curves were averaged over 256 laser pulses. The triplet lifetimes were determined by exponential fitting of the kinetic curves using the OriginPro 7.1.

### 2.3. Syntheses

3-Nitrophthalonitrile **1** and 4-nitrophthalonitrile **2** were synthesized according to literature [20]. 4,4'-Isopropylidenedioxydiphenyl **3** was obtained from commercial suppliers. The syntheses of compounds **5** and **9** has been reported in literature [21]. All solvents were dried and purified as described by Perrin and Armarego [22]. Commercial CHCl<sub>3</sub> was dried with P<sub>2</sub>O<sub>5</sub> then distilled. The distilled CHCl<sub>3</sub> was stored on activated molecular sieves. Purification of commercial DMSO was achieved by drying overnight with chromatographic grade alumina. It are then refluxed for 4 h over CaO, dried over CaH<sub>2</sub>, and then fractionally distilled at low pressure. It was then stored over molecular sieves. Both solvents purified freshly before use. Target precursor **4** was prepared by a nucleophilic aromatic substitution reaction between compound **1** and 4,4'-isopropylidenedioxydiphenyl **3** in DMSO, Scheme 1.

#### 2.3.1. 3,3'-(4,4'-(Propane-2,2-diyl) bis(4,1-phenylene))bis(oxy)diphthalonitrile (**4**)

Compound **3** (2.0 g, 8.67 mmol) was dissolved in dry DMSO (15 mL) and compound **1** (3 g, 17.34 mmol) was added under inert atmosphere. To this reaction mixture finely ground anhydrous

potassium carbonate (2.4 g, 17.3 mmol) was added. After 4 h of stirring at room temperature, further potassium carbonate (0.58 g, 4.3 mmol) was added and this same amount was added again after 24 h of stirring. After a total of 5 days of stirring, the reaction mixture was poured into water (200 mL) resulting in the formation of a white precipitate. The crude product was centrifuged and was further purified by chromatography over a silica gel column using a CHCl<sub>3</sub> as eluent. This process was repeated once. Finally, the pure product was dried using P<sub>2</sub>O<sub>5</sub> for one week. Yield: 2.9 g. IR(KBr) ( $\mu_{\max}/\text{cm}^{-1}$ ): 3078 (Ar–CH), 2228 (C≡N), 1573 (C=C), 1256 (C–O–C). <sup>1</sup>H NMR (DMSO-*d*<sub>6</sub>):  $\delta$ , ppm 7.83 (2H, d,  $J = 7.6$  Hz, Ar–H), 7.37 (2H, d,  $J = 8.8$  Hz, Ar–H), 7.29 (6H, d,  $J = 7.2$  Hz, Ar–H), 7.18 (4H, d,  $J = 8.4$  Hz, Ar–H), 1.69 (6H, s, –CH<sub>3</sub>). Anal. Calc. for C<sub>31</sub>H<sub>20</sub>N<sub>4</sub>O<sub>2</sub>: C, 77.49; H, 4.20; N, 11.66%. Found: C, 77.37; H, 3.68; N, 12.03%.

General procedure for **6–8**: A mixture of complex **4** or **5** (0.10 g, 0.21 mmol) and magnesium(II) chloride (0.3 g, 0.31 mmol) for **6** and **8** or zinc(II) acetate (0.104 g, 0.313 mmol) for **7** (using **4**) was ground in a quartz crucible and heated in sealed glass tube for 15 min under argon atmosphere at 450 °C for MgPcs **6** and **8** and for 12 min under argon atmosphere at 300 °C for ZnPc **7**, respectively. After cooling to room temperature, the green reaction products were washed with hot methanol and hot water. The products were separated by column chromatography on silica gel using chloroform and a gradient of chloroform-methanol up to 50%. And then, the products were washed with methanol, ethanol, acetonitrile and acetone for 24 h, consecutively in the Soxhlet apparatus. Finally, the green products were obtained by column chromatography on silica gel using chloroform as eluting solvent. All of the compounds are soluble in common solvents such as CHCl<sub>3</sub>, dichloromethane, dimethylformamide, and DMSO, and had Mp >350 °C.

#### 2.3.2. 1',11',15',25'-[Tetrakis(4,4'-isopropylidenedioxydiphenyl)]bis-phthalocyaninato dimagnesium(II) (**6**)

Dark green color. Yield: 0.010 g (10%). UV-Vis (CHCl<sub>3</sub>)  $\lambda_{\max}/\text{nm}$  ( $\log \epsilon/\text{dm}^{-3} \text{ mol}^{-1} \text{ cm}^{-1}$ ): 742 (3.72), 700 (4.70), 671 (4.01), 632 (3.97), 320 (4.52). IR[(KBr)  $\mu_{\max}/\text{cm}^{-1}$ ]: 3085 (Ar–CH), 1577 (C=C), 1256 (C–O–C). <sup>1</sup>H NMR (DMSO-*d*<sub>6</sub>):  $\delta$ , ppm 7.85–7.02 (56H, m, Ar–H), 1.72 (24H, m, –CH<sub>3</sub>). Anal. Calc. For C<sub>124</sub>H<sub>80</sub>N<sub>16</sub>O<sub>8</sub>Mg<sub>2</sub>: C,

75.57; H, 4.09; N, 11.37. Found: C, 76.01; H, 4.15; N, 11.45%. MALDI-TOF-MS  $m/z$  Calculated: 1970.67. Found  $[M]^+$ : 1970.82.

### 2.3.3. 1',11',15',25'-[Tetrakis(4,4'-isopropylidenedioxydiphenyl)]bis-phthalocyaninato dizinc(II) (**7**)

Green color. Yield: 0.012 g (11%). UV-Vis ( $\text{CHCl}_3$ )  $\lambda_{\text{max}}/\text{nm}$  ( $\log \epsilon/\text{dm}^{-3} \text{mol}^{-1} \text{cm}^{-1}$ ): 743 (3.92), 699 (4.56), 669 (3.93), 630 (3.87), 320 (4.64). IR[(KBr)  $\mu_{\text{max}}/\text{cm}^{-1}$ ]: 3078 (Ar-CH), 1579 (C=C), 1245 (C-O-C).  $^1\text{H}$  NMR (DMSO- $d_6$ ):  $\delta$ , ppm 7.85–7.01 (56H, m, Ar-H), 1.70 (24H, m, -CH<sub>3</sub>). Anal. Calc. For  $\text{C}_{124}\text{H}_{80}\text{N}_{16}\text{O}_8\text{Zn}_2$ : C, 72.55; H, 3.93; N, 10.92. Found: C, 71.92; H, 3.88; N, 10.93%. MALDI-TOF-MS  $m/z$  Calculated: 2052.88. Found  $[M-4\text{H}]^+$ : 2048.49.

### 2.3.4. 2',10',16',24'-[Tetrakis(4,4'-isopropylidenedioxydiphenyl)]bis-phthalocyaninato dimagnesium(II) (**8**)

Dark green color. Yield: 0.012 g (12%). UV-Vis ( $\text{CHCl}_3$ )  $\lambda_{\text{max}}/\text{nm}$  ( $\log \epsilon/\text{dm}^{-3} \text{mol}^{-1} \text{cm}^{-1}$ ): 685 (4.33), 670 (3.97), 619 (3.71), 350 (4.36). IR[(KBr)  $\mu_{\text{max}}/\text{cm}^{-1}$ ]: 3064 (Ar-CH), 1587 (C=C), 1238 (C-O-C).  $^1\text{H}$  NMR (DMSO- $d_6$ ):  $\delta$ , ppm 7.76–6.95 (56H, m, Ar-H), 1.70 (24H, m, -CH<sub>3</sub>). Anal. Calc. For  $\text{C}_{124}\text{H}_{80}\text{N}_{16}\text{O}_8\text{Mg}_2$ : C, 75.57; H, 4.09; N, 11.37. Found: C, 75.68; H, 4.37; N, 11.39%. MALDI-TOF-MS  $m/z$  Calculated: 1970.67. Found  $[M]^+$ : 1969.996.

## 2.4. Photophysical studies

### 2.4.1. Fluorescence quantum yields

Fluorescence quantum yields ( $\Phi_F$ ) were determined by the comparative method [23,24], Eq. (1):

$$\Phi_F = \Phi_{F(\text{Std})} \frac{F \cdot A_{\text{Std}} \cdot n^2}{F_{\text{Std}} \cdot A \cdot n_{\text{Std}}^2} \quad (1)$$

where  $F$  and  $F_{\text{Std}}$  are the areas under the fluorescence curves of **6–9** and the standard, respectively.  $A$  and  $A_{\text{Std}}$  are the respective absorbances of the sample and standard at the excitation wavelengths (which was  $\sim 0.05$  in all solvents used), and  $n$  and  $n_{\text{Std}}$  are the refractive indices of solvents used for the sample and standard, respectively. ZnPc ( $\Phi_F = 0.20$ ) was employed as the standard [25].

### 2.4.2. Triplet quantum yields and lifetimes

The solutions for triplet quantum yields and lifetimes were introduced into a 1.0 mm pathlength UV-Visible spectrophotometry cell, deaerated using nitrogen and irradiated at the Q-band maxima. Triplet state quantum yields ( $\Phi_T$ ) of **6–9** were determined by the triplet absorption method [26] using zinc phthalocyanine (ZnPc) as a standard; Eq. (2):

$$\Phi_T = \Phi_T^{\text{Std}} \cdot \frac{\Delta A_T \cdot \epsilon_T^{\text{Std}}}{\Delta A_T^{\text{Std}} \cdot \epsilon_T} \quad (2)$$

where  $\Delta A_T$  and  $\Delta A_T^{\text{Std}}$  are the changes in the triplet state absorbances of **6–9** and the standard, respectively.  $\epsilon_T$  and  $\epsilon_T^{\text{Std}}$  are the triplet state molar extinction coefficients for **6–9** and the standard, respectively.

$\Phi_T^{\text{Std}}$  is the triplet quantum yield for the standard, ZnPc ( $\Phi_T = 0.65$  in DMSO) [27].  $\epsilon_T$  and  $\epsilon_T^{\text{Std}}$  were determined from the molar extinction coefficients of their respective ground singlet state ( $\epsilon_S$  and  $\epsilon_S^{\text{Std}}$ ) and the changes in absorbances of the ground singlet states ( $\Delta A_S$  and  $\Delta A_S^{\text{Std}}$ ), and excited triplet states ( $\Delta A_T$  and  $\Delta A_T^{\text{Std}}$ ) according to Eq. (3):

$$\epsilon_T = \epsilon_S \cdot \frac{\Delta A_T}{\Delta A_S} \quad (3)$$

Quantum yields of internal conversion ( $\Phi_{\text{IC}}$ ) were obtained from Eq. (4), which assumes that only three processes (fluorescence, intersystem crossing and internal conversion), jointly deactivate the excited singlet state of the **6–9** molecules.

$$\Phi_{\text{IC}} = 1 - (\Phi_F + \Phi_T) \quad (4)$$

## 3. Results and discussion

### 3.1. Syntheses and characterization

The syntheses of bisphthalodinitriles **4** and **5** is based on the reaction of **3** with excess of compound **1** or **2** in dry DMSO in the presence of  $\text{K}_2\text{CO}_3$  as a base, at room temperature in good yields. The ball-type binuclear Mg(II)Pc and Zn(II)Pc complexes **6–8** were prepared as a mixture of isomers by the reaction of compound **4** or **5** with  $\text{MgCl}_2$  or  $\text{Zn}(\text{CH}_3\text{COO})_2$ . Complex **9** was synthesized as reported before [21]. Cyclotetramerization of the phthalonitrile derivative **4** or **5** to the MPc derivatives **6–8** was accomplished without a solvent in the presence of metal salts at 300 °C for **7** and 450 °C for **6** and **8**. Column chromatography on silica gel using  $\text{CHCl}_3$  as mobile phase was used twice to purify the complexes. The structure and purity of the MgPc and ZnPc derivatives was confirmed by UV-Vis,  $^1\text{H}$  NMR, IR and mass spectral data and elemental analyses.

The IR spectrum of **4** clearly indicates the absence of OH groups of **3**. A diagnostic feature of the formation of **6–8** from the phthalodinitrile derivatives **4** and **5**, is the disappearance of the sharp CN vibration of the latter at 2228 and 2232  $\text{cm}^{-1}$ , respectively.

The  $^1\text{H}$  NMR spectra of **4** shows the aromatic protons between 7.87 and 7.26 ppm, integrating for a total of 20 for protons. In the  $^1\text{H}$  NMR spectrum of **4**, a sharp singlet signal was observed at 1.69 ppm belonging to  $\text{CH}_3$ . The  $^1\text{H}$  NMR spectra of Pcs **6–8**, were recorded in DMSO, and were similar to each other. The aromatic protons appeared at 7.85–7.02, 7.85–7.01 and 7.76–6.95 ppm as well as  $\text{CH}_3$  groups at 1.72, 1.70 and 1.70 ppm, respectively and integrating for a total of 80 for **6–8**. Elemental analysis results also were consistent with the proposed structures of **6–8**. The purified phthalocyanines were further characterized by mass spectra. The expected mass values corresponded with the found values for all complexes using dithranol as the matrix. The results were repeated twice to give the observed molecular peaks. Molecular ion peak for MgPcs and deprotonated molecular ion peak ZnPcs were found. The ion peaks of complexes **6–8** were observed at 1970.82, 2048.49 and

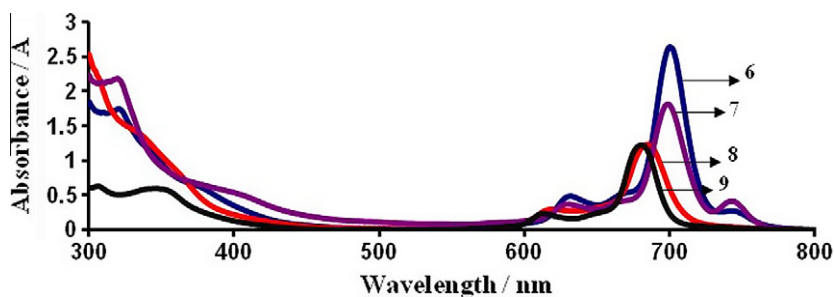


Fig. 1. Absorption spectra of complexes **6–9** in  $\text{CHCl}_3$  at concentration  $5 \times 10^{-5} \text{mol dm}^{-3}$ .

1969.996 amu, respectively. MPC complexes have been observed to degrade with molecular ion peaks  $[M]^+$ ,  $[M+nH]^+$  or  $[M-nH]^+$  (with  $n$  being variable) [28] in some matrices as observed in this work.

The UV–Vis spectra in  $CHCl_3$  shown in Fig. 1 for **6–9** are in accord with the expected structure. The band maxima are listed in Table 1. The phthalocyanines show typical electronic spectra with

**Table 1**

UV–Vis absorption (Q-band), emission and excitation spectral data, and photophysical data for the phthalocyanines.

Solvent	$\lambda_{\max}/nm$ ( $\log \epsilon/dm^{-3} mol^{-1} cm^{-1}$ )								
	CHCl <sub>3</sub>	DMSO							
Complex	$\lambda_{Abs}$	$\lambda_{Abs}$	$\lambda_{Ems}$	$\lambda_{Exc}$	$\Delta\lambda_{Stokes}$	$\Phi_F$	$\Phi_T$	$\Phi_{IC}$	$\tau_T$ ( $\mu s$ )
<b>6</b>	700(4.70)	698	709	699	11	0.14	0.84	0.02	510
<b>7</b>	699(4.59)	697	707	698	10	0.11	0.88	0.01	310
<b>8</b>	685(4.33)	682	692	683	10	0.22	0.62	0.16	910
<b>9</b>	682(4.56)	680	691	682	11	0.15	0.74	0.11	350

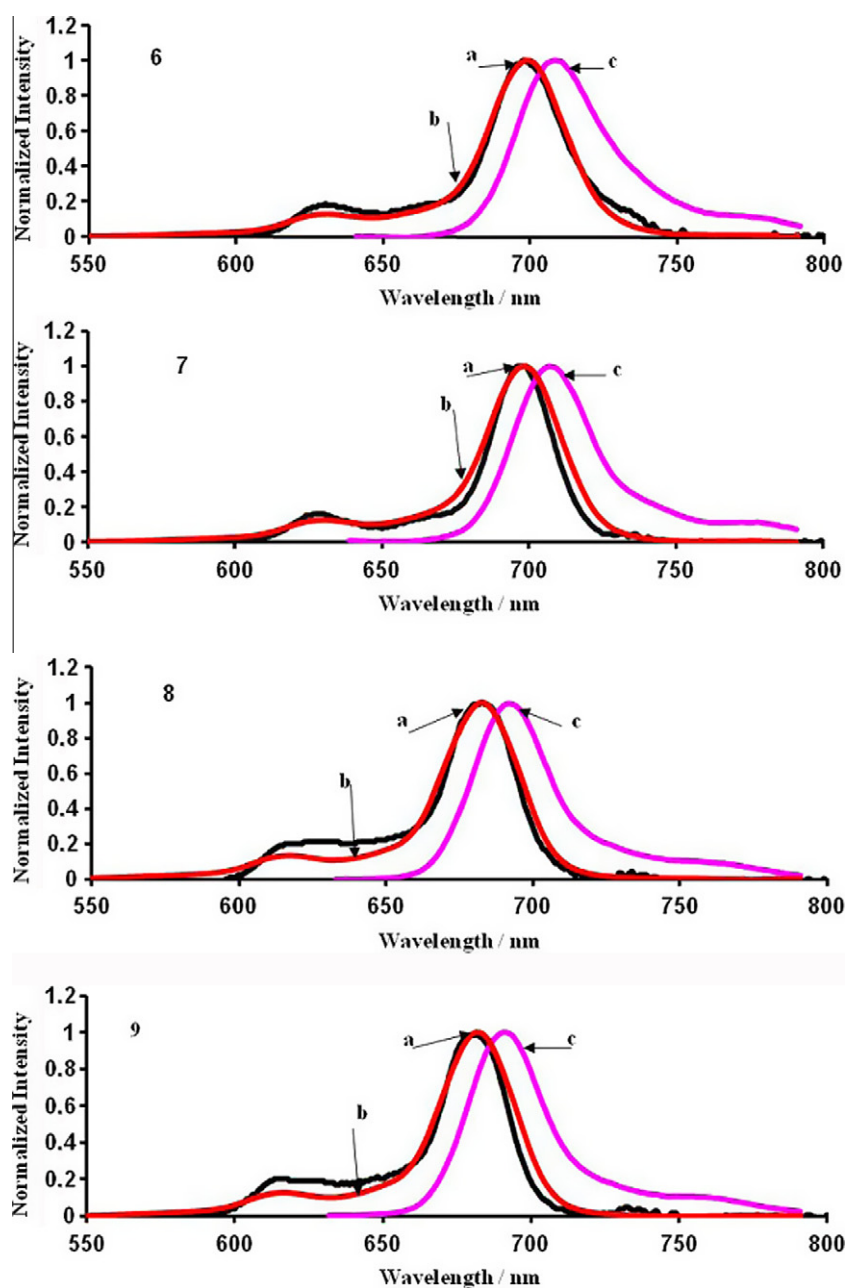


**Fig. 2.** Absorbance (a), excitation (b), emission (c) spectra of complexes **6–9** in DMSO, Excitation  $\lambda_{\max}$  = 614, 620, 622, 613 nm, respectively.

two absorption regions, one in the UV region at about 300–400 nm (B-band) and the other in the visible region at 600–700 nm (Q-band). Aggregation behavior of Pc is a result of coplanar association of rings progressing from monomer to dimer and higher order complexes and it is dependent on concentration, nature of solvent and substituents, metal ions and temperature [29]. Aggregation in MPcs is observed as a broadened or split Q-band, with the high energy band being due to the aggregate and the low energy band due to the monomer. Complexes **6** and **7** show Q-band absorptions at 698 nm, 697 nm whereas complexes **8** and **9** show Q-bands absorption at 682 nm, 680 nm in DMSO, Table 1. In CHCl<sub>3</sub>, complexes **6** and **7** show Q-band absorption at 700 and 699 nm, whereas complexes **8** and **9** show Q-band absorption at 685 and 682 nm, respectively, Table 1 and Fig. 1. This red shift in complexes **6** and **7** is due to substitution at non-peripheral position. It is well known that  $\alpha$  substitution results in red shifting of the spectra [30,31]. Complexes **6–9** show B-bands from 320 to 337 nm. However, complexes **6** and **7** in CHCl<sub>3</sub> has an extra band near 742 and 743 nm, which could be associated with a loss of symmetry often observed in chlorinated solvents [32]. The observation of the extra band in chloroform is due to protonation since this solvent may contain small amounts of acid as observed before [33]. This extra band is not observed in DMSO. The broad shoulder observed at 632, 630, 619, 613 nm for **6–9**, respectively, in chloroform has been reported to indicate aggregation of complexes of ball-type structure [17–19].

A well defined band near 620 nm in ball-type phthalocyanines is due to exciton coupling between the two Pc rings [17]. The spectra of complexes **6** to **9** in DMSO shows bands in this region, which may be attributed to intermolecular interactions between the rings in agreement with literature. However, there is more broadening for **8** and **9** which are peripherally substituted, due to aggregation. Non-peripheral substitution prevents aggregation to a larger extent compared to peripheral substitution. Thus it is clear that there is more aggregation for complexes **8** and **9** which are peripherally substituted compared to non-peripherally substituted **6** and **7**, as is typical of phthalocyanines [31].

### 3.2. Fluorescence spectra and quantum yields

The absorption, fluorescence excitation and emission spectra of complex **6–9** in DMSO are shown in Fig. 2. The excitation, absorption and emission spectral data are listed in Table 1. The absorption and excitation spectra show the same Q-band maxima, however, the absorption spectra are broadened in the 600–650 nm region for **8** and **9** compared to the emission and excitation spectra, due to aggregation. The proximity of the wavelength of each component of the Q-band absorption to the Q-band maxima of the excitation spectra for all complexes suggests that the nuclear configurations of the ground and excited states are similar and not affected by excitation. The emission spectra are mirror images of the excitation spectra. Stokes shifts were 10 or 11 nm, typical of ZnPc complexes [32]. The effect of point of substitution is not clear from the nature of excitation and emission spectra.

The fluorescence quantum yield ( $\Phi_F$ ) values are typical of MPc complexes for MgPc and ZnPc derivatives (**6–9**). The  $\Phi_F$  values ranged from 0.11 to 0.22 in DMSO. The  $\Phi_F$  values were lower for ZnPc derivatives than for MgPc derivatives. This is attributed to the central Zn metal which is heavier than Mg and hence encourages intersystem crossing to the triplet state as will be confirmed below. Face-to-face interaction of the two monomers in dimers is expected to decrease the energy gap between the singlet state and the triplet state and enhance the formation of triplet state (i.e. intersystem crossing increases) decreasing fluorescence [34]. However, in this work the  $\Phi_F$  values are similar to those of

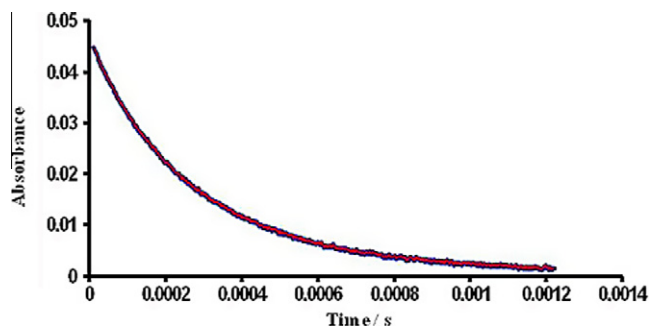


Fig. 3. Triplet state decay curve of complex **7** in DMSO.

monomeric phthalocyanines, showing the interaction between the two rings is minimal.

### 3.3. Triplet quantum yields and lifetimes

The triplet quantum yields ( $\Phi_T$ ) and lifetimes of the complexes are listed in Table 1 and Fig. 3 shows the triplet decay curve for the complex **7** (in DMSO) which obeyed second order kinetics. Triplet quantum yields represent the fraction of absorbing molecules that undergo intersystem crossing to the metastable triplet excited state.

High  $\Phi_T$  values and correspondingly low  $\Phi_F$  values are observed for ZnPc derivatives compared to MgPc counterparts substituted at same positions, due to a more efficient intersystem crossing (ISC), for the former complexes. The  $\Phi_T$  values for **6–9** are 0.84, 0.88, 0.62 and 0.74, respectively. The  $\Phi_T$  values are higher for the non-peripherally substituted derivatives **6** and **7** compared to their peripherally substituted derivatives **8** and **9**, due to reduced aggregation in the former.

Complexes **6–9** have low  $\Phi_{IC}$  values, which may be explained by strong intramolecular interactions between the Pc rings, probably due to the cofacial structure. All complexes showed reasonably long triplet lifetimes with  $\tau_T$  ranging from 310 to 910  $\mu$ s. MgPc derivatives **6** and **8** show longer  $\tau_T$  when compared to ZnPc derivatives **7** and **9**, due to the heavy atom effect of Zn. Non-peripheral substitution in **7** shows slightly shorter  $\tau_T$  values compared to peripheral substitution in **9** for ZnPc derivatives, hence showing a small effect of position of the substituent on the triplet lifetime values. However, comparing MgPc complexes **8** with **6** shows a large effect of peripheral substitution on triplet lifetimes. The  $\tau_T$  values are much longer for peripheral (**8**) compared to non-peripheral (**6**) substitution in MgPc derivatives.

## 4. Conclusions

The syntheses of the ball-type Mg(II)Pc and Zn(II)Pc complexes **6–8** and photophysical properties of complexes **6–9** are presented. MgPc derivatives **6** and **8** show longer  $\tau_T$  when compared to corresponding ZnPc derivatives **7** and **9**. The largest triplet yields were observed for the non-peripherally substituted complexes **6** and **7**, showing that non-peripheral substitution favors increased population of the triplet state. All complexes show reasonably high triplet state quantum yields and long triplet life which are required for efficient photosensitization.

## Acknowledgments

This work was supported by the Department of Science and Technology (DST) and National Research Foundation (NRF), South Africa through DST/NRF South African Research Chairs Initiative

for Professor of Medicinal Chemistry, Nanotechnology, the Research Fund of the Yildiz Technical University (Project No: 24-01-02-12) and Rhodes University.

## References

- [1] J. Simon, P. Bassoul (Eds.), *Design of Molecular Materials: Supramolecular Engineering*, Wiley, Chichester, 2000, p. 197.
- [2] M.A. Diaz Garcia, I. Ledoux, J.A. Duro, T. Torres, F. Agullo-Lopez, J. Zyss, *J. Phys. Chem.* 98 (1994) 8761.
- [3] H. Eichhorn, D. Wöhrle, D. Pressner, *Liq. Cryst.* 22 (1997) 643.
- [4] J.D. Wright, P. Roisin, G.P. Rigby, R.J.M. Nolte, M.J. Cook, S.C. Thorpe, *Sens. Actuators B* 13 (1993) 276.
- [5] I. Okura, *Photosensitization of Porphyrins and Phthalocyanines*, Kodansha Ltd. and Gordon and Breach Science Publishers, Tokyo, 2000, pp. 45.
- [6] R. Bonnett, *Chemical Aspects of Photodynamic Therapy*, Gordon and Breach Science, Amsteldijk, The Netherlands, 2000, pp. 199.
- [7] T. Nyokong, in: J. Zagal, F. Bedioui, J.P. Dodelet (Eds.), *N4-macrocyclic Metal Complexes*, vol. 18, Springer, New York, 2006, p. 63.
- [8] R. Zhou, F. Josse, W. Gopel, Z.Z. Ozturk, O. Bekaroğlu, *Appl. Organomet. Chem.* 10 (1996) 557.
- [9] D. Wöhrle, L. Kreienhoop, G. Schnurpfeil, J. Elbe, B. Tennigkeit, S. Hiller, D. Schlettwein, *J. Mater. Chem.* 5 (1995) 1819.
- [10] E. Ben-Hur, in: B.W. Henderson, T.J. Dougherty (Eds.), *Photodynamic Therapy*, Marcel Dekker, New York, 1992, p. 63.
- [11] C.M. Allen, W.M. Sharman, J.E. van Lier, *J. Porphyrins Phthalocyanines* 5 (2001) 161.
- [12] H. Kolarova, P. Nevrelava, R. Bajgar, *Toxicol. in Vitro* 21 (2007) 249.
- [13] E. Ben-Hur, W.S. Chan, in: K.M. Kadish, K.M. Smith, R. Guillard (Eds.), *Porphyrin Handbook, Phthalocyanine and Materials*, vol. 19, Academic Press, New York, 2003, p. 1 (chapter 117).
- [14] A.C. Tedesco, J.C.G. Rotta, C.N. Lunardi, *Curr. Org. Chem.* 7 (2003) 187.
- [15] A.Y. Tolbin, A.V. Ivanov, L.G. Tomilova, N.S. Zefirov, *Mendeleev Commun.* 12 (2002) 96.
- [16] A.Y. Tolbin, A.V. Ivanov, L.G. Tomilova, N.S. Zefirov, *J. Porphyrins Phthalocyanines* 7 (2003) 162.
- [17] O. Bekaroglu, in: J. Jiang (Ed.), *Functional Phthalocyanine Molecular Materials, Structure and Bonding*, vol. 135, Springer, New York, 2010, p. 105.
- [18] Z. Odabaşı, F. Dumludağ, A.R. Özkaya, S. Yamauchi, N. Kobayashi, O. Bekaroğlu, *Dalton Trans.* 39 (2010) 8143.
- [19] Z. Odabaşı, I. Koc, A. Altındal, A.R. Özkaya, B. Salih, O. Bekaroglu, *Synth. Met.* 160 (2010) 967.
- [20] B.N. Achar, G.M. Fohlen, J.A. Parker, J. Keshavayya, *Polyhedron* 6 (1987) 1463.
- [21] M. Canlıca, A. Altındal, A.R. Özkaya, B. Salih, O. Bekaroglu, *Polyhedron* 27 (2008) 1883.
- [22] D.D. Perrin, W.L.F. Armarego, *Purification of Laboratory Chemicals*, second ed., Pergamon Press, Oxford, 1980.
- [23] S. Fery-Forgues, D. Lavabre, *J. Chem. Ed.* 76 (1999) 1260.
- [24] J. Fu, X.Y. Li, D.K.P. Ng, C. Wu, *Langmuir* 18 (2002) 3843.
- [25] A. Ogunsipe, J.Y. Chen, T. Nyokong, *New J. Chem.* 7 (2004) 822.
- [26] P. Kubát, J. Mosinger, *J. Photochem. Photobiol. A Chem.* 96 (1996) 93.
- [27] T.H. Tran-Thi, C. Desforge, C.C. Thiec, *J. Phys. Chem.* 93 (1989) 1226.
- [28] A.Y. Tolbin, V.E. Pushkarev, G.F. Nikitin, L.G. Tomilova, *Tetrahedron Lett.* 50 (2009) 4848.
- [29] H. Engelkamp, R.J.M. Nolte, *J. Porphyrins Phthalocyanines* 4 (2000) 454.
- [30] M.J. Stillman, T. Nyokong, in: C.C. Leznoff, A.B.P. Lever (Eds.), *Phthalocyanines: Properties and Applications*, vol. 1, VCH, New York, 1989 (chapter 3).
- [31] T. Nyokong, H.J. Isago, *J. Porphyrins Phthalocyanines* 8 (2004) 1083.
- [32] W. Chidawanyika, A. Ogunsipe, T. Nyokong, *New J. Chem.* 31 (2007) 377.
- [33] M. Durmuş, T. Nyokong, *Spectrochim. Acta A* 69 (2008) 1170.
- [34] J. Ren, X.L. Zhao, Q.C. Wang, C.F. Ku, D.H. Qu, C.P. Chang, H. Tian, *Dyes Pigments* 64 (2005) 179.